Molecular Imaging
Volume 16 : 1-10

DOI: 10.1177/1536012116689499
journals.sagepub.com/home/mix
SAGE

Targeted Imaging of Tumor-Associated Macrophages by Cyanine 7-Labeled Mannose in Xenograft Tumors

Chong Jiang, MD[1], Huawei Cai, PhD[1], Xiaodong Peng, MD[2], Ping Zhang, PhD[3], Xiaoai Wu, PhD[1], and Rong Tian, MD[1]

Abstract

Mannose receptor is considered as a hallmark of M2-oriented tumor-associated macrophages (TAMs), but its utility in TAMs was rarely reported. Therefore, deoxymannose (DM), a high-affinity ligand of mannose receptor, was labeled with near-infrared dye cyanine 7 (Cy7), and its feasibility of targeted imaging on TAMs was evaluated in vitro and in vivo. The Cy7-DM was synthesized, and its binding affinity with induced TAMs in vitro, whole-body imaging in xenograft tumor mouse model in vivo, and the cellular localization in dissected tissues were evaluated. We demonstrated a high uptake of Cy7-DM by induced M2 macrophages and TAMs in tumor tissues. In vivo near-infrared live imaging visualized abundant TAMs in tumor lesions instead of inflammatory sites by Cy7-DM imaging, and the quantity of Cy7-DM signals in tumors was significantly higher than that shown in inflammatory sites from 1 to 8 hours of imaging. Our results suggest that mannose could rapidly and specifically target TAMs and is a promising candidate for targeted diagnosis of tumor with rich TAMs.

Keywords

tumor-associated macrophage, mannose receptor, inflammation, near-infrared imaging

Introduction

Tumor-associated macrophages (TAMs) are important components of the tumor stromal microenvironment and function in tumor development, tissue invasion, metastasis, immune suppression, angiogenesis, and lymph angiogenesis.[1–5] Preclinical and clinical studies have shown satisfactory outcomes with treatment by targeting TAMs to inhibit tumor burden and metastasis in breast, melanoma, renal, prostate, cervical, lung, liver, pancreatic, brain, squamous cell, and ovarian cancers with high levels of TAMs.[6–13]

Macrophages have varied activation pathways and immune functions. The M1 macrophages are activated by classical immune signal pathways and function to remove pathogens and tumor cells.[14] However, M2 macrophages, when activated by T-helper 2 (Th2) cytokines, promote release of vascular endothelial growth factors, which promote tumor growth and metastasis.[2,3,15] Tumor-associated macrophages have the same characteristics as M2 macrophages, including production of marginal interleukin 12 (IL-12), enhanced IL-10, and expression of high levels of mannose receptors (MRs). Tumor-associated macrophages are therefore considered as a distinct M2-polarized population of M2 macrophages.[8–10]

Mannose receptors are transport proteins that have multiple C-type lectin-like domains that transport mannose, fucose, and *N*-acetyl glucosamine into cells.[16] Mannose receptors are expressed in macrophages that live in the red pulp of the spleen, the paracortex of the lymph node, and the cortex of the thymus. Furthermore, MRs are highly expressed on the surface of TAMs, but there are few MRs on the surface of M1 macrophages.[9,17–19]

Molecular imaging using agents targeted to TAMs offers a noninvasive and quantitative method for assessing the presence and density of these cells. Leimgruber and colleagues and

[1] Department of Nuclear Medicine, West China Hospital, Sichuan University, Chengdu, China
[2] Department of Clinical Immunology, West China Hospital, Sichuan University, Chengdu, China
[3] State Key Laboratory of Oral Diseases, West China Hospital of Stomatology, Sichuan University, Chengdu, China

Submitted: 22/05/2015. Revised: 01/12/2016. Accepted: 03/12/2016.

Corresponding Author:
Rong Tian, Department of Nuclear Medicine, West China Hospital, Sichuan University, Chengdu 610000, China.
Email: rongtiannuclear@126.com

Melancon and colleagues bolstered the concept of TAM-targeted imaging using nanoparticle and macromolecular contrast agents.[20–22] Melancon et al stated that PG-Gd-NIR813 is an indicator for the presence of TAMs and may be used to track TAMs in vivo. They also stated that the poly (L-glutamic acid) (PG) moiety of their probe can specifically target TAMs. However, they did not indicate what characteristic of the PG-M2 interaction makes this a specific interaction.[20]

There are several studies which have indicated that the MR is a specific target for imaging TAMs because there is overexpression of MR on TAMs.[20–24] A few studies have been reported for TAM imaging targeting the MR. Mannose-coated liposome was used as a carrier of ^{64}Cu for positron emission tomography imaging of lung cancer in a mouse model.[25] ^{99m}Tc-labeled anti–macrophage MR (MMR) microantibody was used for single-photon emission computed tomography imaging of breast cancer in a mouse model, and uptake was found to be high in the TAM-enriched tumor.[22] ^{18}F-labeled camelid single-domain antibody fragments were demonstrated to specifically target the MMR.[26] The shortcoming of radionuclide-labeled probes is that in vivo live imaging and ex vivo histological imaging cannot be conducted with the same probe. Moreover, preparations of liposomes and antibodies are relatively costly.

Fluorescence imaging has been widely used to study various diseases because of advantages including high sensitivity and nonradioactive properties. Sun et al prepared a CD206-targeting Near-Infrared Fluorescence (NIRF) imaging agent, DyLight680–antibody conjugate (Dye-anti-CD206), and demonstrated that NIRF imaging using this agent would allow noninvasive imaging of TAMs in vivo in a breast cancer mouse model.[24] However, preparations of these antibodies are relatively costly.

Mannose can combine with the MR with high affinity,[9] and it is easy to procure. Cy7.SE has been widely applied in the labeling and detection of proteins, antibodies, nucleic acids, and other biological molecules. In the present study, we labeled mannose with a near-infrared fluorescent dye, Cy7, and explored its capability to image TAMs in cell culture and in a live mouse model.

Materials and Methods

Cells and Reagents

Mouse-derived macrophage cell line Ana-1 and the human hepatoma cell line SMMC-7721 were purchased from China Center for Type Culture Collection, Chinese Academy of Sciences (Wuhan, Hubei, China). The cells were cultured with RPMI-1640 medium containing 10% fetal bovine serum, 1% penicillin, and streptomycin in a cell culture incubator at 37°C with 5% carbon dioxide. Cy7-N-hydroxysuccinimide ester (Cy7.SE), D-mannosamine hydrochloride, lipopolysaccharide (LPS), interferon γ (IFN-γ), IL-4, and IL-13 were purchased from Sigma-Aldrich (St Louis, Missouri). Monoclonal antibodies for CD206, CD16, and F4/80 were purchased from Abcam (Cambridge, United Kingdom).

Synthesis of Cy7-D-mannosamine

The compound Cy-7-D-mannosamine (Cy7-DM) was prepared from commercially available D-mannosamine hydrochloride (Supplementary Figure S1). Cy7-N-hydroxysuccinimide ester (0.8 mg; 1 μmol) was conjugated to the terminal amino group of D-mannosamine hydrochloride (1.8 mg; 10 μmol) in a 1:1 mixture (0.5 mL) of acetonitrile and sodium borate buffer (0.1 mol/L; pH 8.5). After it was stirred at 4°C for 2 hours in the dark, the reaction mixture was placed in room temperature storage for 1 hour. The products were isolated and purified by semipreparative, reverse-phase high-performance liquid chromatography (HPLC; Venusil XBP C18, Agela, USA; Capricorn P1050 HPLC pump, Goebel, DE; and Capricorn UV1000D detector, Goebel, DE). The mobile phase changed from 60% solvent A (0.1% trifluoroacetic acid in water) and 40% solvent B (0.1% trifluoroacetic acid in 80% aqueous acetonitrile) to 100% solvent B during 30 minutes at a flow rate of 3 mL/min. The ultraviolet detector was set to 215 nm for the experiments.[27] Mass spectral (MS) data were acquired on a Waters Q-TOF Premier mass spectrometer in university (Micromass, Manchester, United Kingdom). The HPLC-purified Cy7-DM was used for further experiments.

Cell Induction and MR Detection

Macrophage induction was performed as described previously.[25,28,29] Ana-1 cells were inoculated in 6-well plates (1×10^6 cells per well) and divided into 2 groups. Mouse IL-4 (20 ng/mL) and IL-13 (20 ng/mL) were added to the first group for TAM polarization induction, whereas LPS (100 ng/mL) and IFN-γ (20 ng/mL) were added to the second group for M1 polarization induction. After 48-hour induction, macrophage polarization was evaluated with flow cytometry. In brief, the cells (5×10^6 cells) in microplate wells were trypsinized with 0.25% trypsin and incubated with TAM-distinctive anti-CD206 antibody (fluorescein isothiocyanate [FITC] labeled) or M1-distinctive anti-CD16 antibody (phycoerythrin labeled) at 4°C for 30 minutes, respectively. After incubation, the cells were washed twice with phosphate-buffered saline (PBS) to remove dissociated antibodies and resuspended with 300 μL of Dulbecco PBS buffer for flow cytometry. Then, 5×10^6 induced macrophages in 1 mL of medium were added with 1 nmol Cy7-DM and incubated at 37°C for 0.5 hours. After a PBS washing process, the binding frequency of Cy7-DM with induced M1 macrophages and TAMs was also evaluated by flow cytometry.

Animal Model and Live Imaging

All of the protocols used in this report were approved by the University Animal Care and Use Committee. A mouse xenograft tumor model was established with SMMC-7721 human hepatoma cells. Cells (2×10^6 cells in 0.1 mL PBS) were injected subcutaneously at the right axilla of nude mice. The tumor size was measured daily with a caliper, and tumor

volume was calculated (volume = length × width × width/2). The SMMC-7721 human hepatocellular tumors were excised from these mice for histology. The inflammation model was established by intramuscularly injecting 0.2 mL of telepine oil (Sigma-Aldrich) into the right leg. At 48 hours postinjection, marked local swelling appeared at the injected leg, indicating induced inflammation. The inflammatory tissue was excised from these mice for histology.

For optical imaging, mice were anesthetized with 2% isoflurane, and Cy7-DM (2 nmol in 100 μL) was injected intravenously via the tail vein. In vivo animal fluorescence imaging was performed for 0.8 seconds of exposure at 5 minutes, 1 hour, 2 hours, 4 hours, 6 hours, and 8 hours postinjection with excitation of 745 nm and emission of 800 nm using the IVIS Spectrum in vivo imaging system (PerkinElmer, Santa Clara, California). For the blocking group, 100 nmol of unlabeled mannose was intravenously injected to mice before 1 hour prior to Cy7-DM injection before scanning. Fluorescence intensity of each mouse was measured by drawing regions of interest on the well boundaries and recorded these as average radiance (p/s/cm^2/sr) using LiveImage software v.3.2. The mice were killed after the imaging process, and tissues were collected for Cy7-DM uptake analysis with immunofluorescence detection.

Immunohistochemical Assay

Tumors and inflammatory tissues were dissected and fixed with 4% paraformaldehyde. Fixed tissues were sectioned as 5-μm slices using a Leica CM3050 cryostat (Leica Microsystems, Buffalo Grove, Illinois), and 2 adjacent sections were separated into 2 groups for each examination. Samples in group 1 were preblocked with 10% goat serum for 1 hour and added with mouse anti-CD206 primary antibody (1:500) overnight at 4°C and Alexa Fluor594-bound antimouse immunoglobulin G (IgG) secondary antibody (1:750) for 1 hour at room temperature (Life Technologies, Carlsbad, California). After a washing procedure with PBS to remove nonspecific bound antibody, FITC-labeled antihuman F4/80 antibody (Abcam ab204266, diluted as 1:100) was added for 1-hour incubation at room temperature under dark conditions. Slices were then stained with 4′,6-diamidino-2-phenylindole (DAPI) for nucleus localization and sealed with glycerol buffer for further detection. Samples in group 2 were stained with mouse anti-CD16 antibody, Alexa Fluor594-bound antimouse IgG secondary antibody, FITC antihuman F4/80 antibody, and DAPI as described earlier. All sections (groups 1 and 2) were scanned using a laser confocal scanning microscope (Olympus FV1000, Japan).

Statistics

Statistical analyses were conducted using the Student *t* test assuming unequal variances. The *P* values of the Student *t* test were adjusted by Holm procedure because of the multiple comparisons. The R environment and the multitest package were used for statistical analyses and generation of graphs. A *P* value of .05 was considered statistically significant.

Results

Synthesis of Cy7-DM

The schematic structure of Cy7-DM is presented in Figure 1A. Cy-7-D-mannosamine was synthesized and purified by reverse-phase HPLC. The retention times of Cy7-DM and Cy7-SE were 2.29 and 3.05 minutes. The chemical purity of Cy7-DM was higher than 95% after purification (Figure 1B and C). The conjugate identity was confirmed by electrospray mass spectrometry under condition of MS *m/z* (Electrospray Ionization [ESI]): 262.1 $[M + H]^+$. The measured molecular weight for Cy7-DM was 897, which fits well to its theoretic molecular weight 895.92.

Induction of Macrophage Polarization

The induced Ana-1 macrophages were observed under an optical microscope to evaluate the morphological changes. The macrophages that were induced by IL-4 and IL-13 were found be smaller and rounder with less adhesion capability than non-induced macrophages, and these induced macrophages had high refraction and lacked pseudopodia, features that are typical of TAMs (Figure 2B). However, the macrophages induced by LPS and IFN-γ had long spindles and slender pseudopodia, features typical of M1 macrophages as described previously[30] (Figure 2C).

The surface-specific antigens of different polarized macrophages on induced cells were evaluated by flow cytometry. After respective incubation with M1 and TAM distinctive antibodies, the binding frequency of the CD206 antibody to macrophages induced by IL-4 and IL-13 was 95.0%, and the CD16-positive frequency was only 8.7%, which is consistent with TAMs (Figure 2D). In contrast, the macrophages induced by LPS and IFN-γ had specific binding affinity of 99.5% to CD16 antibody but only 0.6% to CD206 antibody, which is consistent with M1 macrophages (Figure 2E). These results indicated a successful induction of TAMs by combined treatment with IL-4 and IL-13.

The binding affinities of Cy7-DM to induced M1 macrophages and TAMs are presented in Figure 2F. Binding affinity result showed that Cy7-DM had significantly higher uptake in the induced TAMs (97.0% by gate) than that binding frequency in the induced M1 macrophages (2.4% by gate), which indicated that the targeting potential of Cy7-DM for TAMs was suitable.

Cyanine-7-D-Mannosamine Imaging of TAMs In Vivo

Targeted imaging of Cy7-DM in TAMs in live animals was performed using an optical IVIS imaging system that allowed the kinetic visualization and drug clearance in the same animal. A total of 30 nude mice with SMMC-7721 hepatoma tumor xenograft or inflammatory muscles were randomly allocated into the experimental tumor group, the blocking tumor group,

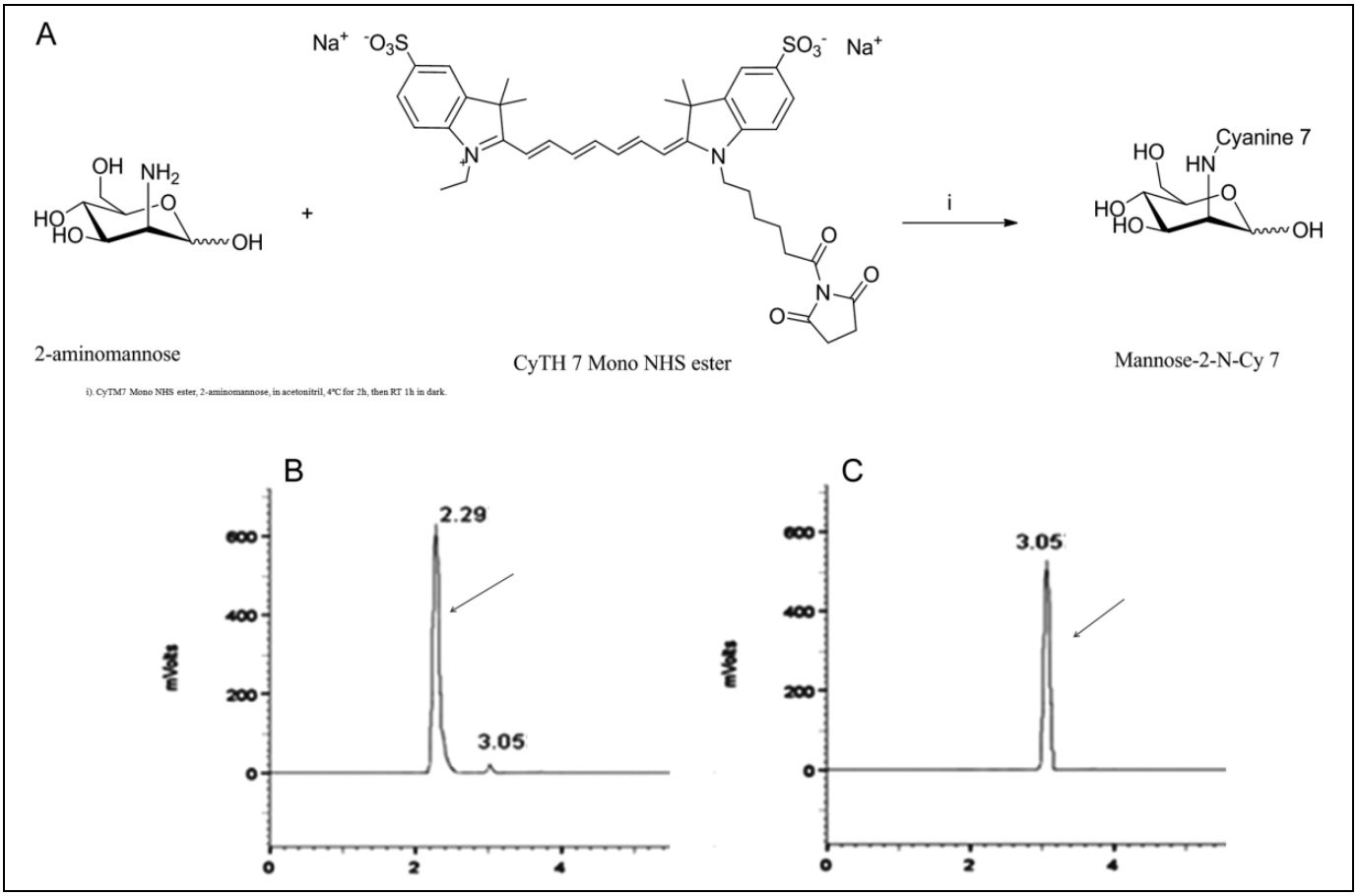

Figure 1. Schematic structure and high-performance liquid chromatography (HPLC) profile of synthesized cyanine 7 deoxymannose (Cy7-DM). A, Schematic structure and synthesis method of Cy7-DM. B, High-performance liquid chromatography profile of Cy7-DM and Cy7-SE. The arrows denote the retention time of Cy7-DM (2.29 minutes) and unbound Cy7-SE (3.05 minutes).

and the experimental inflammation group. After injection of Cy7-DM (approximate 2 nmol), mice were scanned from 5 minutes to 8 hours. The visible results demonstrated clear systemic circulation of Cy7-DM agent within 5 minutes post-injection of subsequent excretion into the bladder. The Cy7-DM progressively accumulated in the tumor and inflammatory sites of the mice from 1 hour throughout 8 hours (Figure 3A). Receptor blockage with nonlabeled mannose (100 nmol) prior to Cy7-DM injection effectively inhibited the accumulation of fluorescent signals at tumor sites throughout the scan (Figure 3A). The radiant efficiencies of the Cy7-DM signal were quantitatively analyzed with Living Image 4.2 software (PerkinElmer), and the mean fluorescent intensities are presented in Figure 3C, indicating that signals in tumors were higher than those in sites of inflammation ($P < .05$).

The biodistribution evaluation of Cy7-DM in individual tissues showed similar results; the intensity of signals from high to low in tissues was tumor > stomach > lung > spleen > kidney > intestine > brain > liver > inflammatory tissue (Figure 4A and B). All of these findings suggest that Cy7-DM is a specific marker for tumors with abundant TAMs.

Tissues dissected from SMMC-7721 tumor xenograft and inflamed muscles were stained with macrophage-denoting antibody (anti-F4/80), M1 macrophages antibody (anti-CD16), TAM antibody (anti-CD206), and nucleus indicator dye (DAPI). Immunofluorescence results demonstrated that staining of CD206 antibody was perfectly colocalized with the signal of F4/80 antibody in tumor tissue, indicating that macrophages were majority of TAMs in tumors (Figure 5A and B). However, in inflammatory tissue, there was marked overlap of positive tissue staining with CD16 antibody and F4/80 antibody, suggesting the presence of M1 macrophages in inflammatory tissues (Figure 5D and E).

The specific binding potential of Cy7-DM to tumor and inflammatory tissues was also analyzed by multiple immunofluorescent staining. The significant overlap of Cy7-DM was observed with CD206 signals in tumor tissue, but rarely in inflammatory tissue, suggesting that Cy7-DM specifically binds to TAMs in tumor tissues (Figure 5C) instead of M1 macrophages in inflammatory organs (Figure 5F).

Discussion

Tumor-associated macrophages are recruited to most tumors and play an important role in tumor growth. Extensive infiltration of tumors by TAMs is closely associated with tumor

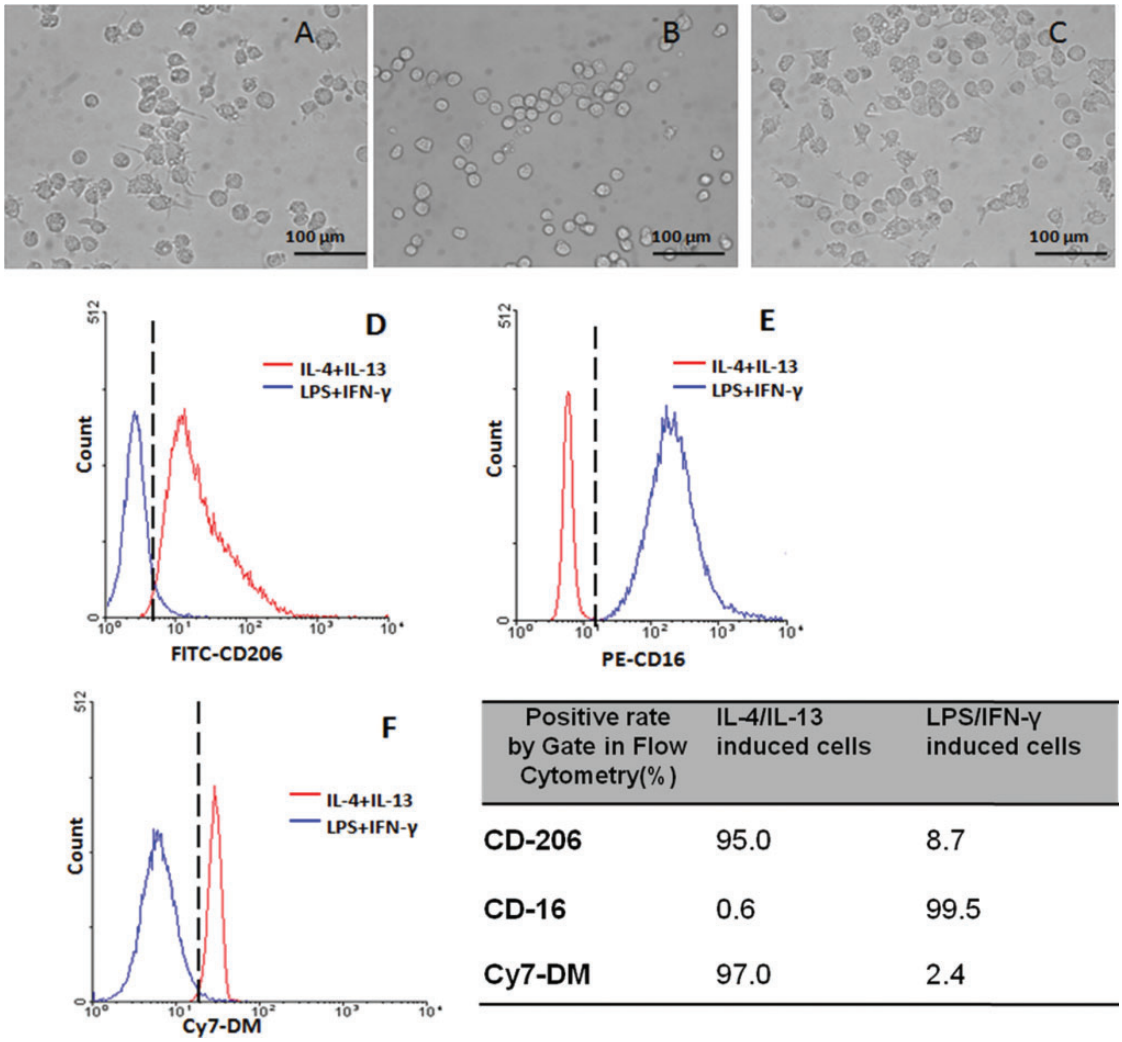

Positive rate by Gate in Flow Cytometry(%)	IL-4/IL-13 induced cells	LPS/IFN-γ induced cells
CD-206	95.0	8.7
CD-16	0.6	99.5
Cy7-DM	97.0	2.4

Figure 2. Induction of polarized M1 and M2 macrophages and the evaluation of their binding affinity with Cy7-DM. A, Noninduced mouse macrophage Ana-1 cells (×100). B, Interleukin 4- and interleukin 13-induced Ana-1 cells at 48 hours postinduction (×100). C, Lipopolysaccharide- and interferon γ-induced Ana-1 cells at 48 hours postinduction (×100). D, Tumor-associated macrophage (M2 macrophage) distinctive antigen CD206 was detected in individually polarized Ana-1 macrophages. E, M1 macrophage distinctive antigen CD16 was detected in individually polarized Ana-1 macrophages. F, Binding affinity evaluation of Cy7-DM with M2 and M1 macrophages. Black dotted lines denote the gates in flow cytometry analysis.

occurrence. However, targeted imaging of TAMs in vivo is still limited by lack of proper biomarkers. Mannose receptors are found to be highly expressed on M2-oriented tumor macrophages that are polarized by anti-inflammatory molecules such as IL-4, IL-13, and IL-10 in established tumor xenografts.[28,31] So, the utility of mannose in MR-positive TAM-targeted imaging was evaluated in vitro and in vivo.

In the present study, the expression level of MR in macrophages was externally induced to differentiate into M1 and M2 macrophages,[25,29] and the verification of cell subtype was performed by testing its characteristic expression of CD16 and CD206, respectively. Previous studies have shown that M1 macrophages have high expression of CD16 and low expression of CD206 on the cell surface, whereas M2 macrophages express high number of CD206 and express low number of CD16.[9,19,32,33] Our results showed that the binding frequency of M2 macrophages and M1 macrophages was consistent with prior studies. Finally, the specific binding frequency of Cy7-DM to M2 macrophages was found to be similar to the frequency of CD206 antibody, suggesting that Cy7-DM is a reliable compound for the detection of M2 macrophages in vitro.

M1 macrophages bound significantly less Cy7-DM than M2 macrophages. This finding is likely related to the significantly lower levels of MR expression by M1 cells. It has been reported that IFN-γ, while stimulating phagocytosis by M1 macrophages, downregulates MRs.[34] Therefore, the significantly higher binding potential of Cy7-DM to tumors compared with sites of inflammation on the immunofluorescence assay implies that TAMs are mostly M2 macrophages with high numbers of MRs, while macrophages at sites of inflammation

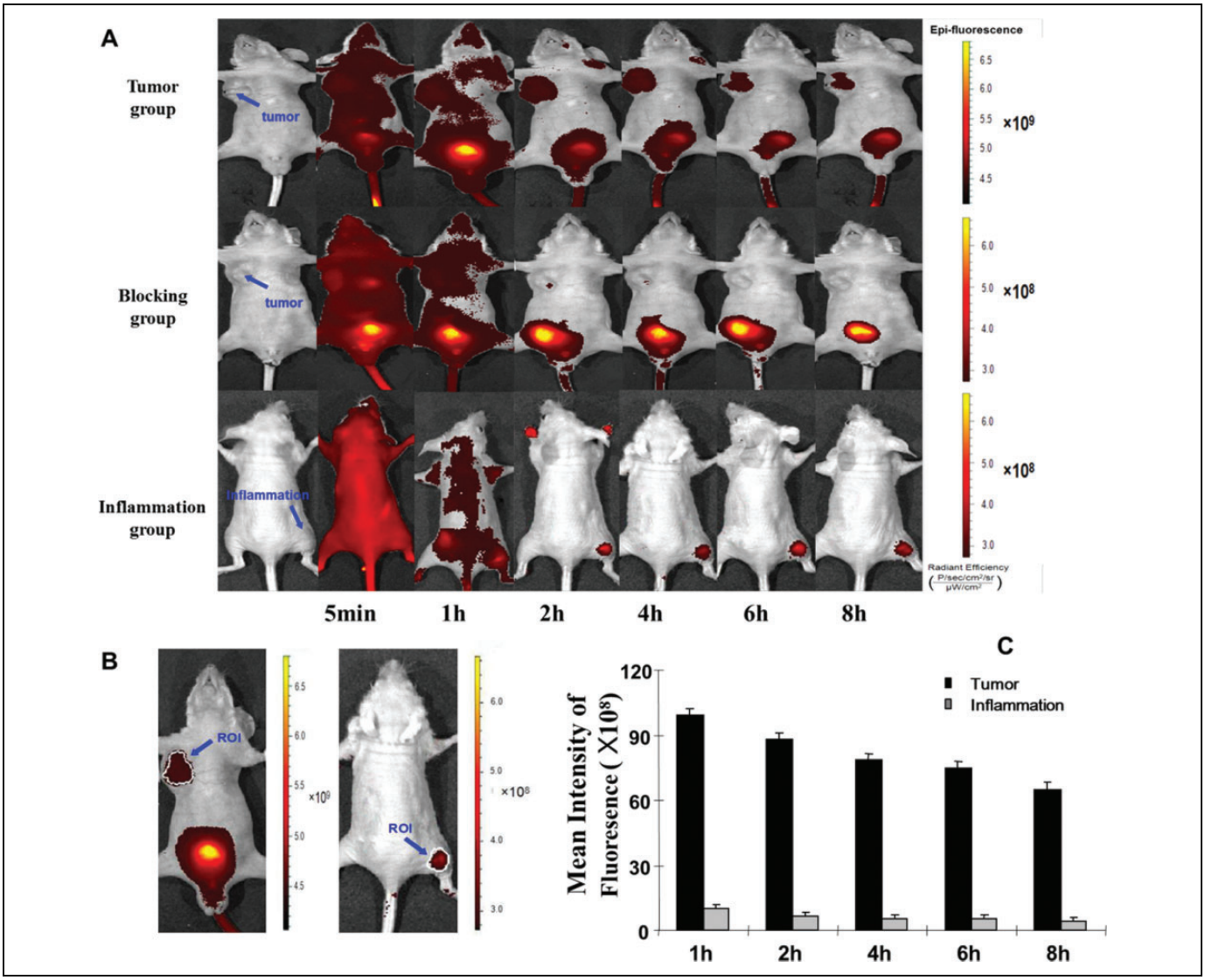

Figure 3. In vivo near-infrared imaging of xenograft tumors by cyanine 7 deoxymannose (Cy7-DM). Cyanine 7 deoxymannose was intravenously injected to mice with hepatoma tumor or inflammatory muscles, and whole-body live imaging was carried out at different time points. One competitive inhibition group of tumor xenograft tumor mice was preinjected with 100 nmol unlabeled mannose 1 hour prior to Cy7-DM injection and imaged at same time points. A, Near-infrared, whole-body images obtained at 5 minutes, 1 hour, 2 hours, 4 hours, 6 hours, and 8 hours postinjection. B, Detailed Cy7-DM live imaging results of mice with tumor or inflammation at 4 hours post injection. C, Fluorescence intensities of Cy7-DM in tumors and inflammatory muscles at different time points.

have lower numbers of M2 macrophages, most likely some combination of M1 and M2 macrophages.[8]

The live animal images demonstrate that Cy7-DM uptake in the tumor is significantly higher than in other organs and tissues, including inflammatory muscle. Again, this is likely because the TAMs are mostly M2 macrophages, while inflammatory tissue contains predominantly M1 macrophages. However, confocal images of tumor tissue show that the Cy7-DM staining colocalizes with CD206, which was specific to M2 macrophages. In inflammatory muscle tissue, there was less overall Cy7-DM uptake and lack of overlap with CD16, an M1-specific antigen. Therefore, the fact that tumor tissue contains mostly M2 macrophages and inflammatory tissue contains mostly M1 macrophages may reflect the intercellular milieu. Those findings demonstrate the specificity of Cy7-DM for M2 macrophages and imply that diagnosis or monitoring of tumors as well as distribution of TAMs can be accomplished with Cy7-DM NIRF imaging in small animals.

Although the fluorescence signal in the tumor is higher than that in the inflammation site, the differences are not as big as anticipated. The relatively large fluorescence signal from the inflammation site (Figure 3) might be related to all of the following reasons. First, M1 macrophages expressed little MR and M1 macrophages bound small amounts of Cy-7-DM. Second, there may be nonspecific uptake of Cy-7-DM due to leaky vessels and increased edema at the inflammation site during the in vivo experiments. Third, macrophages are highly interconvertible. Depending on their environment,

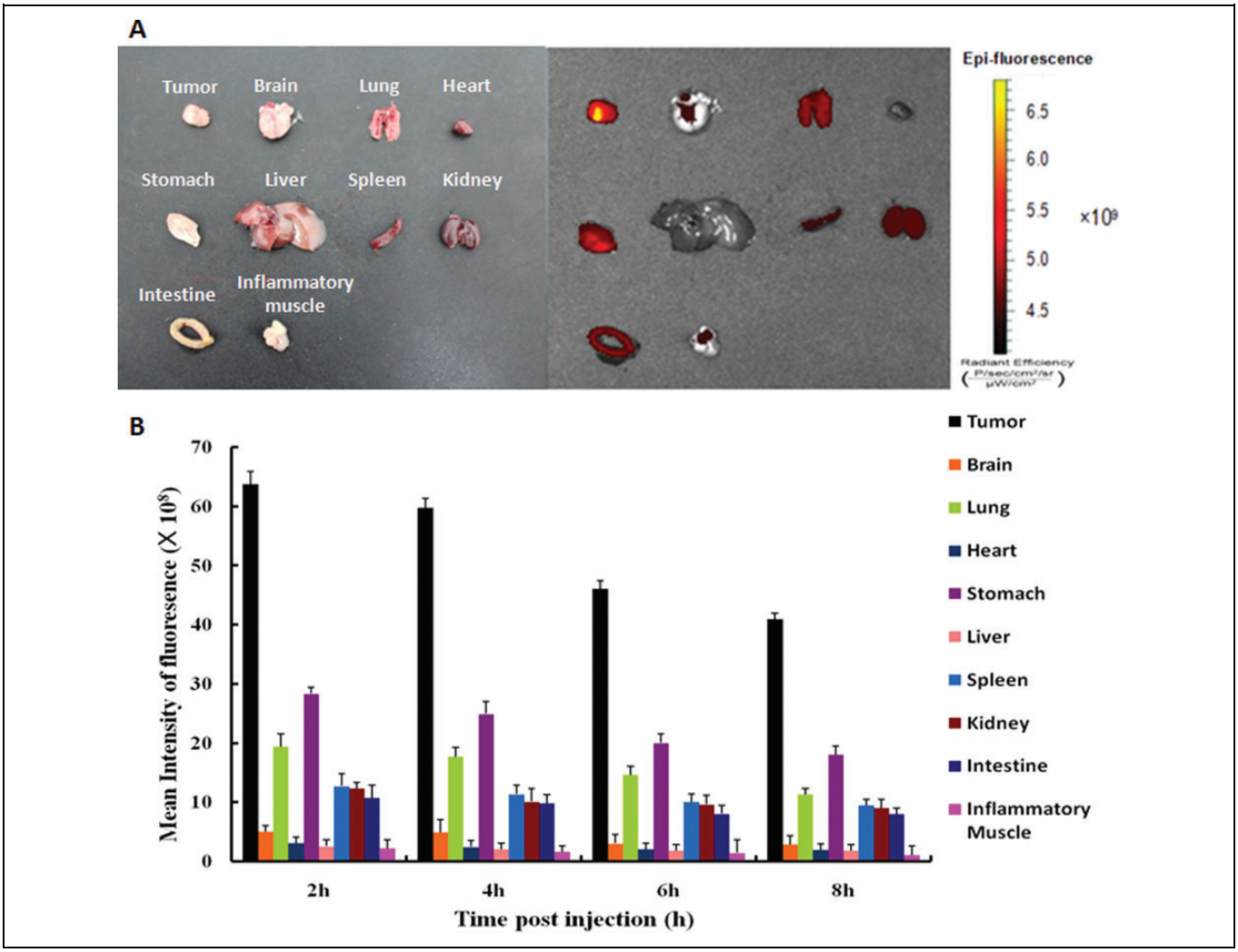

Figure 4. Distribution of cyanine 7 deoxymannose (Cy7-DM) in dissected mouse organs and tissues. A, A total view of different organs dissected from mouse with both tumor and inflammatory muscle at 2 hours post-Cy7-DM injection. B, Fluorescent intensity analysis of organs and tumors at different time points (data reported as mean ± standard deviation [SD]; n = 3 for each time point).

macrophages can transform between the M1 and the M2 states.[31,35–37] Macrophage polarization changes throughout the entire course of infection from baseline to M2 during early infection and then to M1 during late infection.[35] This indicates that the Cy7-DM signal in inflamed tissue may be related to the presence of a small number of TAMs or M2 macrophages.

In this study, we designed an assay to prove that the binding of Cy7-DM to TAMs is a competitive process between receptor and ligand. The cells and mice in the blocking group were administered a 50-fold excess amount of unlabeled mannose before the injection of Cy7-DM. In comparison to the cells and mice that did not receive mannose blockade, these cells or mice showed less uptake of Cy7-DM, suggesting competitive inhibition occurred between mannose and Cy7-DM. Since we have confirmed that binding to the MR is a competitive process, we can therefore consider the possibility that the varied uptake of Cy7-DM observed in the small intestine, lung, spleen, and tumor may have occurred because the resident macrophages in these organs express low levels of MRs.[38]

The Cy7.SE used in the present study is a fluorescent labeling dye and has an excitation wavelength of 747 nm and an emission wavelength of 774 nm. It produces very low absorption background in the near-infrared region. As one of the most stable long-wavelength dyes with high fluorescence intensity, Cy7.SE has been widely applied in the labeling and detection of proteins, antibodies, nucleic acids, and other biological molecules. There are several advantages of using Cy7-DM compared to other probes, especially radionuclide-labeled probes. First, it allows in vivo live imaging and ex vivo histologic imaging to be conducted with the same probe, therefore raising no question about the correlation of vivo live imaging and ex vivo histologic imaging. Second, it is valuable in the real-time monitoring of macrophages in the tumor microenvironment, in facilitating investigations of the cross-talk between

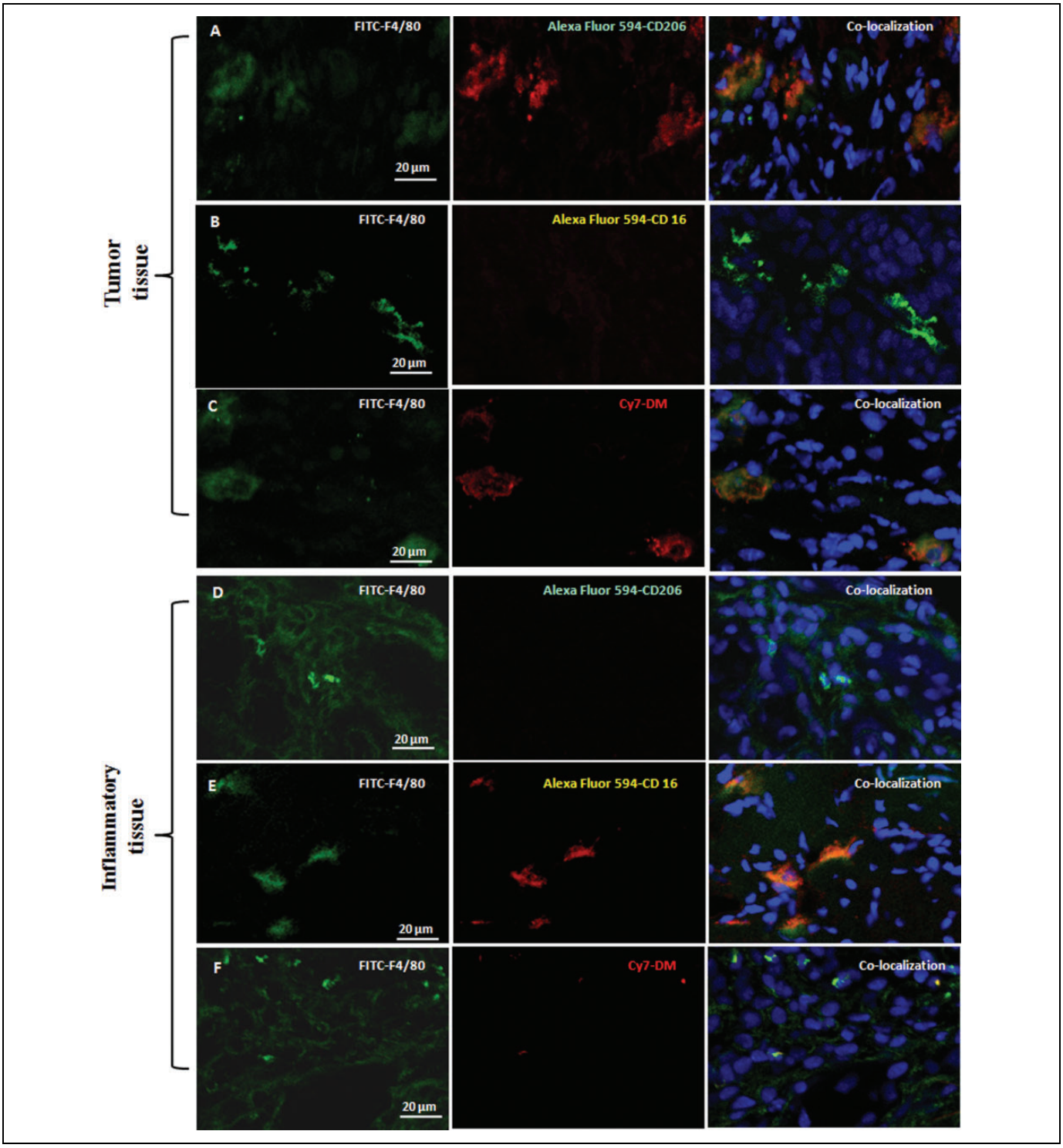

Figure 5. Recognition of TAMs (tumor-associated macrophages) and M1 macrophages in tumor and inflammatory tissues by immunofluorescent imaging. A, F4/80(+) and CD206(+) indicated that TAMs were localized in tumor tissue. B, F4/80(+) and CD16(−) indicated that no M1 macrophages were detected in tumor tissue. C, Cyanine 7 deoxymannose (Cy7-DM) signals were overlapped with macrophages in tumor tissue, Cy7-DM(+) and F4/80(+). D, F4/80(+) and CD206(−) indicated that no TAMs were detected in inflammatory tissue. E, F4/80(+) and CD16(+) indicated that M1 macrophages were localized in inflammatory tissue. F, Merely Cy7-DM signal was found in inflammatory tissue with abundant macrophages.

tumor cells and infiltrating macrophages, in developing new antimacrophage drugs, and in elucidating mechanisms that underlie the development of tumor microenvironments. Third, the conjugation of Cy7 and deoxymannose is simpler and more stable, and the blood clearance is faster than with nanoparticles and antibodies.

Although Cy7.SE is a long-wavelength dye and has better penetration than short-wavelength dyes, Cy7-labeled probes are still limited in the clinic because of tissue attenuation. Therefore, translation of our probe in the clinic may not be an easy task. However, this probe can be useful in preclinical investigations of tumor microenvironment.[39]

Conclusion

In conclusion, the specific binding capability of Cy7-DM to TAMs makes it a potentially useful tool for the diagnosis and monitoring of tumors rich in these cells.

Authors' Note

C. Jiang and H. W. Cai carried out the conjugate synthesis, cell culture, and in vivo imaging works and contributed equally to this project. X. D. Peng and P. Zhang completed the tissue section immunofluorescence. X. A. Wu guided the conjugate synthesis. C. Jiang, H. W. Cai, and R. Tian wrote the manuscript. All the authors have read and approved the final manuscript.

Declaration of Conflicting Interests

The author(s) declared no potential conflicts of interest with respect to the research, authorship, and/or publication of this article.

Funding

The author(s) disclosed receipt of the following financial support for the research, authorship, and/or publication of this article: This research was supported by the National Natural Science Foundation of China (81471693) and the Sichuan Provincial Department of Science and Technology Support Program (2012SZ0005).

Supplemental Material

The online [appendices/data supplements/etc] are available at http://journals.sagepub.com/doi/suppl/10.1177/1536012116689499.

References

1. Obeid E, Nanda R, Fu YX, Olopade OI. The role of tumor-associated macrophages in breast cancer progression (review). *Int J Oncol*. 2013;43(1):5–12.
2. Hao NB, Lu MH, Fan YH, Cao YL, Zhang ZR, Yang SM. Macrophages in tumor microenvironments and the progression of tumors. *Clin Dev Immunol*. 2012;2012:948098.
3. Smith HA, Kang Y. The metastasis-promoting roles of tumor-associated immune cells. *J Mol Med (Berl)*. 2013;91(4):411–429.
4. Ramanathan S, Jagannathan N. Tumor associated macrophage: a review on the phenotypes, traits and functions. *Iran J Cancer Prev*. 2014;7(1):1–8.
5. Riabov V, Gudima A, Wang N, Mickley A, Orekhov A, Kzhyshkowska J. Role of tumor associated macrophages in tumor angiogenesis and lymphangiogenesis. *Front Physiol*. 2014;5:75.
6. Condeelis J, Pollard JW. Macrophages: obligate partners for tumor cell migration, invasion, and metastasis. *Cell*. 2006; 124(2):263–266.
7. Fukuda K, Kobayashi A, Watabe K. The role of tumor-associated macrophage in tumor progression. *Front Biosci (Schol Ed)*. 2012; 4:787–798.
8. Sica A, Schioppa T, Mantovani A, Allavena P. Tumour-associated macrophages are a distinct M2 polarised population promoting tumour progression: potential targets of anti-cancer therapy. *Eur J Cancer*. 2006;42(6):717–727.
9. Mantovani A, Sozzani S, Locati M, Allavena P, Sica A. Macrophage polarization: tumor-associated macrophages as a paradigm for polarized M2 mononuclear phagocytes. *Trends Immunol*. 2002;23(11):549–555.
10. Bronkhorst IH, Ly LV, Jordanova ES, et al. Detection of M2-macrophages in uveal melanoma and relation with survival. *Invest Ophthalmol Vis Sci*. 2011;52(2):643–650.
11. Santoni M, Massari F, Amantini C, et al. Emerging role of tumor-associated macrophages as therapeutic targets in patients with metastatic renal cell carcinoma. *Cancer Immunol Immunother*. 2013;62(12):1757–1768.
12. Panni RZ, Linehan DC, DeNardo DG. Targeting tumor-infiltrating macrophages to combat cancer. *Immunotherapy*. 2013;5(10):1075–1087.
13. Noy R, Pollard JW. Tumor-associated macrophages: from mechanisms to therapy. *Immunity*. 2014;41(1):49–61.
14. Gordon S. Alternative activation of macrophages. *Nat Rev Immunol*. 2003;3(1):23–35.
15. Galdiero MR, Garlanda C, Jaillon S, Marone G, Mantovani A. Tumor associated macrophages and neutrophils in tumor progression. *J cell physiol*. 2013;228(7):1404–1412.
16. Diebold SS, Plank C, Cotten M, Wagner E, Zenke M. Mannose receptor-mediated gene delivery into antigen presenting dendritic cells. *Somat Cell Mol Genet*. 2002;27(1-6):65–74.
17. Madsen DH, Bugge TH. Imaging collagen degradation in vivo highlights a key role for M2-polarized macrophages in extracellular matrix degradation. *Oncoimmunology*. 2013;2(12): e27127.
18. Stahl PD, Ezekowitz RA. The mannose receptor is a pattern recognition receptor involved in host defense. *Curr Opin Immunol*. 1998;10(1):50–55.
19. Movahedi K, Laoui D, Gysemans C, et al. Different tumor microenvironments contain functionally distinct subsets of macrophages derived from Ly6C(high) monocytes. *Cancer Res*. 2010; 70(14):5728–5739.
20. Melancon MP, Lu W, Huang Q, et al. Targeted imaging of tumor-associated M2 macrophages using a macromolecular contrast agent PG-Gd-NIR813. *Biomaterials*. 2010;31(25):6567–6573.
21. Leimgruber A, Berger C, Cortez-Retamozo V, et al. Behavior of endogenous tumor-associated macrophages assessed in vivo using a functionalized nanoparticle. *Neoplasia*. 2009;11(5):459–468, 2 p following 468.
22. Movahedi K, Schoonooghe S, Laoui D, et al. Nanobody-based targeting of the macrophage mannose receptor for effective in vivo imaging of tumor-associated macrophages. *Cancer Res*. 2012;72(16):4165–4177.
23. Zhu S, Niu M, O'Mary H, Cui Z. Targeting of tumor-associated macrophages made possible by PEG-sheddable, mannose-modified nanoparticles. *Mol Pharm*. 2013;10(9):3525–3530.
24. Sun X, Gao D, Gao L, et al. Molecular imaging of tumor-infiltrating macrophages in a preclinical mouse model of breast cancer. *Theranostics*. 2015;5(6):597–608.

25. Locke LW, Mayo MW, Yoo AD, Williams MB, Berr SS. PET imaging of tumor associated macrophages using mannose coated 64Cu liposomes. *Biomaterials*. 2012;33(31):7785–7793.
26. Blykers A, Schoonooghe S, Xavier C, et al. PET imaging of macrophage mannose receptor-expressing macrophages in tumor stroma using 18F-radiolabeled camelid single-domain antibody fragments. *J Nucl Med*. 2015;56(8):1265–1271.
27. Xiao L, Zhang Y, Liu Z, Yang M, Pu L, Pan D. Synthesis of the Cyanine 7 labeled neutrophil-specific agents for noninvasive near infrared fluorescence imaging. *Bioorg Med Chem Lett*. 2010; 20(12):3515–3517.
28. Mosser DM, Edwards JP. Exploring the full spectrum of macrophage activation. *Nat Rev Immunol*. 2008;8(12):958–969.
29. Kittan NA, Allen RM, Dhaliwal A, et al. Cytokine induced phenotypic and epigenetic signatures are key to establishing specific macrophage phenotypes. *PLoS One*. 2013;8(10):e78045.
30. Rey-Giraud F, Hafner M, Ries CH. In vitro generation of monocyte-derived macrophages under serum-free conditions improves their tumor promoting functions. *PLoS One*. 2012; 7(8):e42656.
31. Biswas SK, Sica A, Lewis CE. Plasticity of macrophage function during tumor progression: regulation by distinct molecular mechanisms. *J Immunol*. 2008;180(4):2011–2017.
32. Madsen DH, Leonard D, Masedunskas A, et al. M2-like macrophages are responsible for collagen degradation through a mannose receptor-mediated pathway. *J Cell Biol*. 2013;202(6): 951–966.
33. Jablonski KA, Amici SA, Webb LM, et al. Novel markers to delineate murine M1 and M2 macrophages. *PLoS One*. 2015; 10(12):e0145342.
34. Raveh D, Kruskal BA, Farland J, Ezekowitz RA. Th1 and Th2 cytokines cooperate to stimulate mannose-receptor-mediated phagocytosis. *J Leukoc Biol*. 1998;64(1):108–113.
35. Davis MJ, Tsang TM, Qiu Y, et al. Macrophage M1/M2 polarization dynamically adapts to changes in cytokine microenvironments in *Cryptococcus neoformans* infection. *mBio*. 2013;4(3): e00264–e00213.
36. Buhtoiarov IN, Sondel PM, Wigginton JM, et al. Anti-tumour synergy of cytotoxic chemotherapy and anti-CD40 plus CpG-ODN immunotherapy through repolarization of tumour-associated macrophages. *Immunology*. 2011;132(2): 226–239.
37. Cai X, Yin Y, Li N, et al. Re-polarization of tumor-associated macrophages to pro-inflammatory M1 macrophages by microRNA-155. *J Mol Cell Biol*. 2012;4(5):341–343.
38. Guruvayoorappan C. Tumor versus tumor-associated macrophages: how hot is the link? *Integr Cancer Ther*. 2008;7(2): 90–95.
39. Stoffels I, Dissemond J, Poppel T, Schadendorf D, Klode J. Intraoperative fluorescence imaging for sentinel lymph node detection: prospective clinical trial to compare the usefulness of indocyanine green vs technetium Tc 99m for identification of sentinel lymph nodes. *JAMA Surg*. 2015;150(7): 617–623.